Topographical selective deposition: A comparison between plasma-enhanced atomic layer deposition/sputtering and plasma-enhanced atomic layer deposition/quasi-atomic layer etching approaches

Moustapha Jaffal, Taguhi Yeghoyan, Gauthier Lefèvre, Rémy Gassilloud, Nicolas Possémé, Christophe Vallée, Marceline Bonvalot

Journal of Vacuum Science and Technology A

LETTER | MARCH 24 2021

Topographical selective deposition: A comparison between plasma-enhanced atomic layer deposition/sputtering and plasma-enhanced atomic layer deposition/quasi-atomic layer etching approaches

Special Collection: Special Topic Collection on Area Selective Deposition

Moustapha Jaffal; Taguhi Yeghoyan; Gauthier Lefèvre; Rémy Gassilloud; Nicolas Possémé; Christophe Vallée; Marceline Bonvalot

J. Vac. Sci. Technol. A 39, 030402 (2021)
https://doi.org/10.1116/6.0000969

JVST A
Journal of Vacuum Science & Technology A

LETTER

avs.scitation.org/journal/jva

Topographical selective deposition: A comparison between plasma-enhanced atomic layer deposition/sputtering and plasma-enhanced atomic layer deposition/quasi-atomic layer etching approaches

Cite as: J. Vac. Sci. Technol. A 39, 030402 (2021); doi: 10.1116/6.0000969
Submitted: 6 February 2021 · Accepted: 11 March 2021 ·
Published Online: 24 March 2021

Moustapha Jaffal,[1,a)] Taguhi Yeghoyan,[1] Gauthier Lefèvre,[1] Rémy Gassilloud,[2] Nicolas Possémé,[2] Christophe Vallée,[1,b)] and Marceline Bonvalot[1]

AFFILIATIONS

[1]University Grenoble Alpes, CNRS, CEA/LETI-Minatec, Grenoble INP, LTM, F-38054 Grenoble, France
[2]CEA-LETI, Minatec Campus, F-38054 Grenoble, France

Note: This paper is a part of the Special Topic Collection on Area Selective Deposition.
[a)]**Electronic mail:** moustapha.jaffal@cea.fr
[b)]**Present address:** Colleges of Nanoscale Science and Engineering, SUNY Polytechnic Institute, Albany, NY 12203.

ABSTRACT

In this work, we focus on the development of topographically selective deposition (TSD) leading to local deposition on the vertical sidewalls of 3D structures. A proof of concept is provided for the TSD of Ta_2O_5. The TSD process relies on plasma-enhanced atomic layer deposition (PEALD) alternating with quasi-atomic layer etching (ALE). Quasi-ALE involves a fluorination treatment followed by a directional Ar^+ sputtering step. We show that the fluorination treatment allows a significant decrease in the incident kinetic energy of the subsequent directional Ar^+ sputtering step. Conversely, when no fluorination step is carried out, TSD requires high incident kinetic energies during the directional Ar^+ sputtering step, which, in turn, leads to detrimental plasma-induced damage on horizontal surfaces, such as roughness, also promoting by-product redeposition. The benefits and shortcomings of these two TSD approaches—PEALD/quasi-ALE and PEALD/energetic Ar^+ sputtering—are compared in light of potential bottom-up technological developments.

I. INTRODUCTION

The ongoing pace of device miniaturization, essentially relying on photolithographic techniques, is now gradually reaching its limits for advanced 3D nanoelectronic devices. While Self-Aligned Double Patterning (SADP) is used at the 14 nm pitch, self-aligned quadruple patterning (SAQP) solutions are required beyond the 7 nm node.[1–3] These top-down approaches imply numerous and costly wafer-handling steps during the fabrication process and generate detrimental Edge Placement Errors (EPEs) due to the inherent limitations of photolithography.[4] The traditional top-down miniaturization via multiple patterning is, thus, heading toward a technological bottleneck.[5,6] For this reason, area selective deposition (ASD) has been attracting a lot of attention recently,[7] as a direct bottom-up patterning route for advanced nanoelectronic device fabrication.[8,9] Atomic layer deposition (ALD) is a technique of choice for ASD because it enables growth with atomic-scale thickness control.[10] ASD can be achieved on planar substrates by a prior surface deactivation or surface activation treatment before ALD growth[11,12] or by an appropriate sequencing of deposition and etching steps.[5,13] When dealing with 3D substrates, there is a strong technological interest for the selective coating of either horizontal or vertical surfaces of 3D patterns, leading to a so-called topographical selective deposition (TSD).[14]

In a recent study, our group has developed an original TSD approach for the fabrication of vertical-only coating of 3D substrates based on the alternate combination of a standard PEALD process with an energetic anisotropic Ar^+ sputtering step fully carried out by PEALD in a unique reactor.[15] After a conformal PEALD deposit formed on a 3D substrate, the subsequent anisotropic energetic Ar^+ bombardment step sputter-cleans only horizontal surfaces, because vertical surfaces are not exposed to the incident directional Ar^+ ion flux. We have published a proof of concept of this process, showing the successful selective deposition of 70 nm Ta_2O_5 vertical-only coating in 3D profiles with an aspect ratio of 1:5.[15] This proof of concept was carried out in a unique inductively coupled plasma (ICP) PEALD reactor equipped with an additional RF biasing power supply at the backside of the substrate, which provides tunable Ar^+ ionic bombardment energies. However, a main drawback was identified when this alternate deposition and etch TSD process was transferred to high aspect ratio structures. Indeed, we observed damage on horizontal surfaces, such as amorphization and roughness, as well as by-product redeposition, most likely induced by exposure to energetic Ar^+ bombardment for the horizontal deposit removal.[14]

To address these issues, we have improved this TSD approach to avoid the use of the energetic Ar^+ bombardment step. In this work, this alternate TSD route is described with a proof of concept carried out on 3D substrates to illustrate the selective vertical coating. The obtained results are then compared with our previously published results and discussed in detail.[15]

II. EXPERIMENT

A block diagram of the PEALD setup used in this study is shown in Fig. 1. It consists of a vacuum chamber equipped with an ICP source power operating at 13.56 MHz from Oxford Instruments. Thin film growth is monitored *in situ* using a Film Sense FS-1 multiwavelength ellipsometer for film thickness measurements during growth. *In situ* anisotropic Ar^+ sputtering is enabled by an additional waveform RF substrate biasing kit at the backside of the substrate. The incident kinetic energy of Ar^+ ions impinging on the substrate can then be modulated, thanks to the tunable incident power of the bias (21 W < bias power <100 W).

(Tert-butylimino)tris(dimethylamino) tantalum (TBTDMT) precursor and O_2 plasma are used for the deposition of Ta_2O_5 thin films, according to the recipe described in Fig. 2, leading to a growth per cycle (GPC) of 0.8 Å/cycle. The selective deposition process has first been optimized on planar Si substrates, before being implemented in 3D Si substrates.

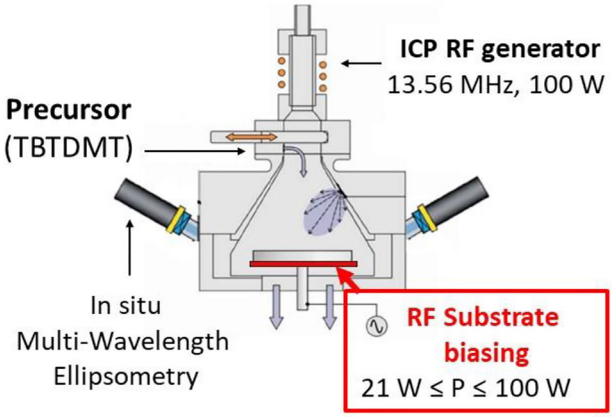

FIG. 1. Block diagram of the PEALD reactor.

III. RESULTS AND DISCUSSION

To mitigate the detrimental effects induced by the high-energy anisotropic Ar^+ bombardment used to remove Ta_2O_5 deposits from horizontal surfaces, we have inserted an intermediate fluorination step just after the Ta_2O_5 conformal thin film deposition. This fluorination treatment consists of a CF_4/H_2 plasma at 100 W and 80 mTorr carried out within the same PEALD reactor chamber (i.e., without any air break) and promotes Ta–F surface bond formation,[16–18] as confirmed from XPS analyses (not shown). Since the Ta–F bond energy (573 ± 13 kJ/mol) is much lower than the Ta–O bond energy (839.7 kJ/mol),[19] the subsequent anisotropic Ar^+ sputtering step can be effective at a much lower incident ionic energy to remove the deposit from surfaces exposed to the ion flux. This, in turn, should minimize damage related to energetic Ar^+ bombardment.

Figure 3 shows the Ar^+ sputtering rate of both as-deposited and fluorinated Ta_2O_5 under a 21 W substrate bias power ($V_{DC} = -140$ V), as evaluated from *in situ* ellipsometric measurements.

It can be seen that the as-deposited Ta_2O_5 film thickness (a) shows a linear decrease corresponding to a constant sputtering rate of 0.15 nm/min. However, fluorinated Ta_2O_5 (b) first exhibits an exponential decrease, followed by a linear trend with a sputtering rate of 0.15 nm/min, similar to case (a). The exponential decrease observed in the initial stages of Ar^+ sputtering indicates an enhanced sputtering efficiency, consistent with weaker surface Ta–F bond formation. However, this enhanced sputtering rate of fluorinated Ta_2O_5 finally reaches a steady-state regime evidenced by the constant etching rate, which becomes identical to that of as-deposited Ta_2O_5. This is taken as a time indication for the

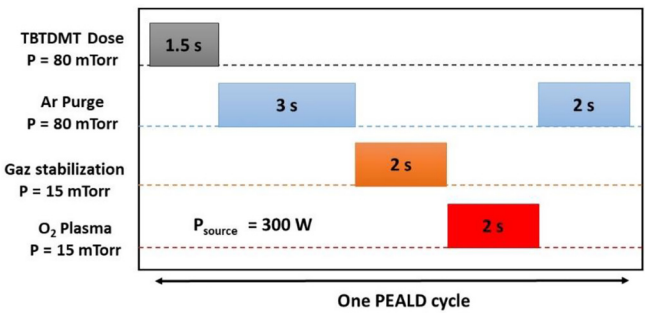

FIG. 2. Experimental parameters of one PEALD cycle for the deposition of Ta_2O_5 thin films.

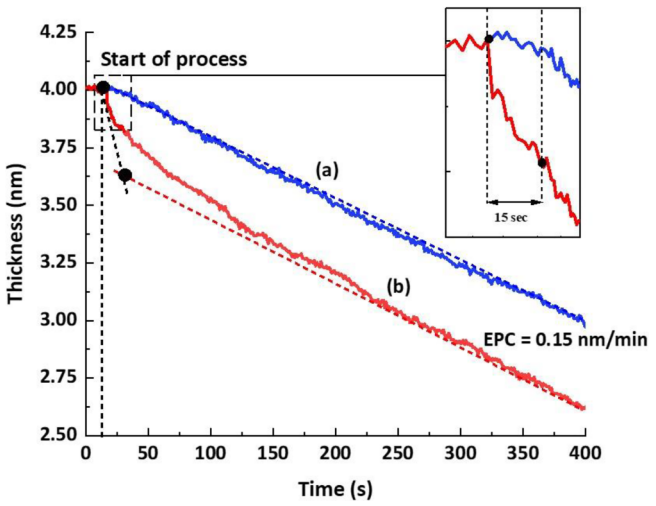

FIG. 3. *In situ* thickness measurements of Ta_2O_5 exposed to a 21 W bias Ar^+ bombardment (V_{DC} = −140 V): (a) as-deposited Ta_2O_5 by PEALD and (b) fluorinated Ta_2O_5 by a 10 s, 100 W CF_4/H_2 plasma exposure.

complete removal of fluorinated surface layers opening access to Ta_2O_5 but also underlines that the 21 W Ar^+ bombardment step is not self-limited. Indeed, no detectable selectivity is observed between the removal of fluorinated and as-deposited Ta_2O_5, respectively, in contrast to conventional atomic layer etching processes. For this reason, this surface fluorination followed by anisotropic Ar^+ sputtering is instead referred to as a quasi-ALE step. We believe that a lower bias power would most likely be more adequate for the selective removal of fluorinated Ta_2O_5 versus pure Ta_2O_5. Unfortunately, the substrate polarization kit setup in our PEALD reactor does not allow bias power values less than 21 W, therefore limiting the current process under development.

Figure 4(a) summarizes the experimental parameters for each of the two steps defining the one quasi-ALE cycle. The CF_4/H_2 fluorination plasma step under 100 W source power is limited to 10 s only, because *in situ* ellipsometric measurements [Fig. 4(b)] show that the thickness levels off beyond this duration, indicating surface saturation by fluorine species. Moreover, the Ar^+ sputtering step has been performed only for 15 s, in order to ensure complete removal of fluorinated Ta_2O_5 and to simultaneously limit plasma-induced damage. This corresponds to a net removal of 0.1 nm of as-deposited Ta_2O_5 [Fig. 4(b)].

We have estimated the degree to which this quasi-ALE process approaches an ideal ALE, as suggested by Kanarik *et al.*[20] The results are shown in Fig. 5, where the synergy between the fluorination and the directional Ar^+ bombardment steps was calculated as follows:[21]

$$S_{quasi-ALE}(\%) = \frac{EPC_{quasi-ALE} - (ER_{fluorination} + ER_{Ar\,sputtering})}{EPC_{quasi-ALE}} \times 100\%. \quad (1)$$

In this formula, $EPC_{quasi-ALE}$ stands for the etch rate per cycle of the quasi-ALE step, as defined in Fig. 4(a); $ER_{fluroination}$ is the etch rate of fluorinated Ta_2O_5; and $ER_{Ar\ sputtering}$ is the etch rate of as-deposited Ta_2O_5 during the anisotropic Ar^+ sputtering step.

This synergy factor is a way of quantifying the degree of cooperative interactions taking place during the two-step quasi-ALE process, as compared with each of the two steps considered separately.[22] An *S* value of 100% would indicate that each step constitutive of the quasi-ALE process and carried out separately is totally ineffective to remove Ta_2O_5. It appears that the 66% synergy

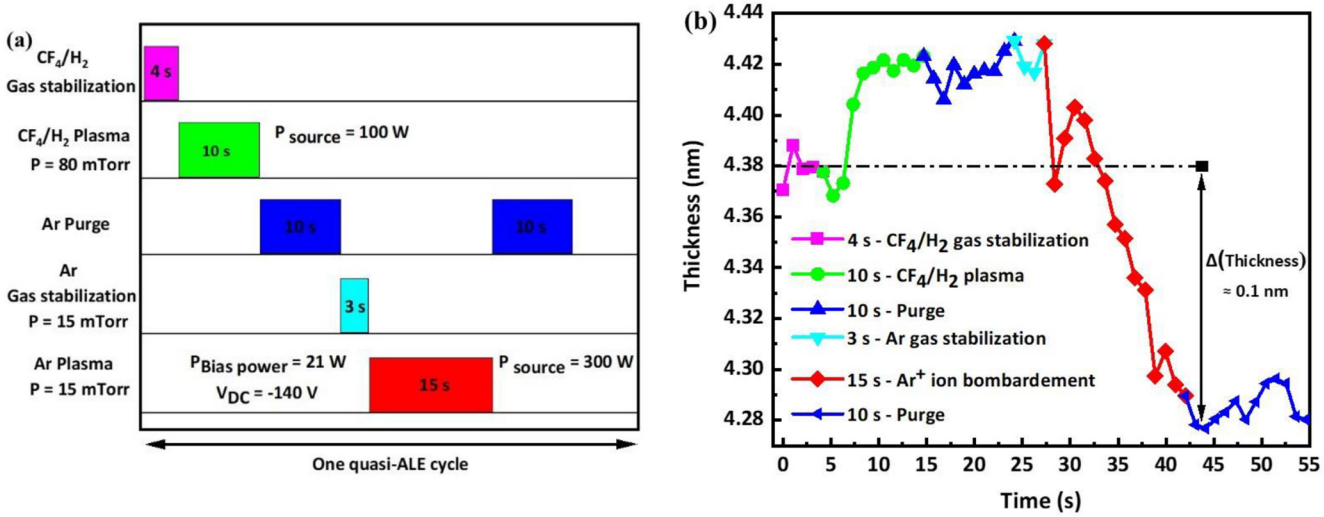

FIG. 4. (a) Experimental parameters of the complete quasi-ALE process step. (b) *In situ* ellipsometric measurements during one quasi-ALE process step.

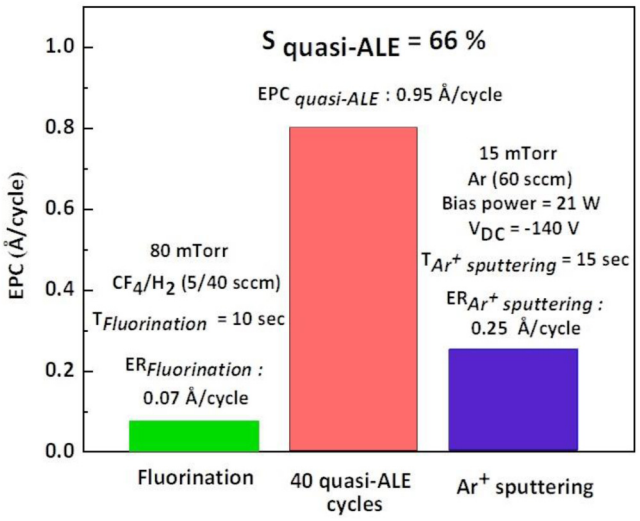

FIG. 5. Estimate of the synergy factor S of the quasi-ALE process defined in Fig. 4(a). The methodology developed by Kanarik *et al.* (Ref. 20) was followed.

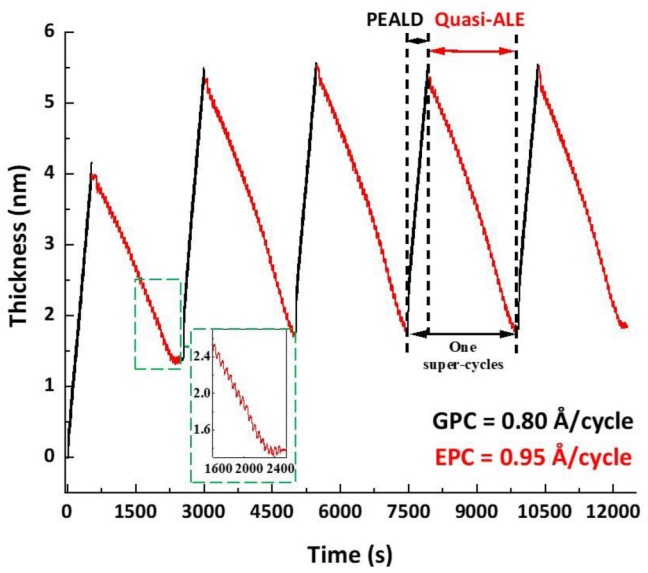

FIG. 6. *In situ* measurements of five Ta_2O_5 PEALD and quasi-ALE super-cycles on a planar Si substrate.

obtained in this work (Fig. 5) is among the lowest values reported in Ref. 20. Since the synergy correlates with the self-limiting aspect of surface reactions, the relatively low S value somehow reflects the poor selectivity of the ion bombardment step in the removal of fluorinated Ta_2O_5 versus the pure Ta_2O_5 surface layers, as mentioned above. Self-limiting reactions are a key asset in both ALD and ALE because they are essential for the control of processes at the atomic scale: the sequencing of self-limiting reactions guarantees that each one of them stops rightaway when reactants released in the previous step are totally consumed.[23] In this regard, we believe that the self-limited character requirement for ALE processes can be challenged by developing kinetically controlled process steps, hence the name quasi-ALE for the TSD process at stake in this study.

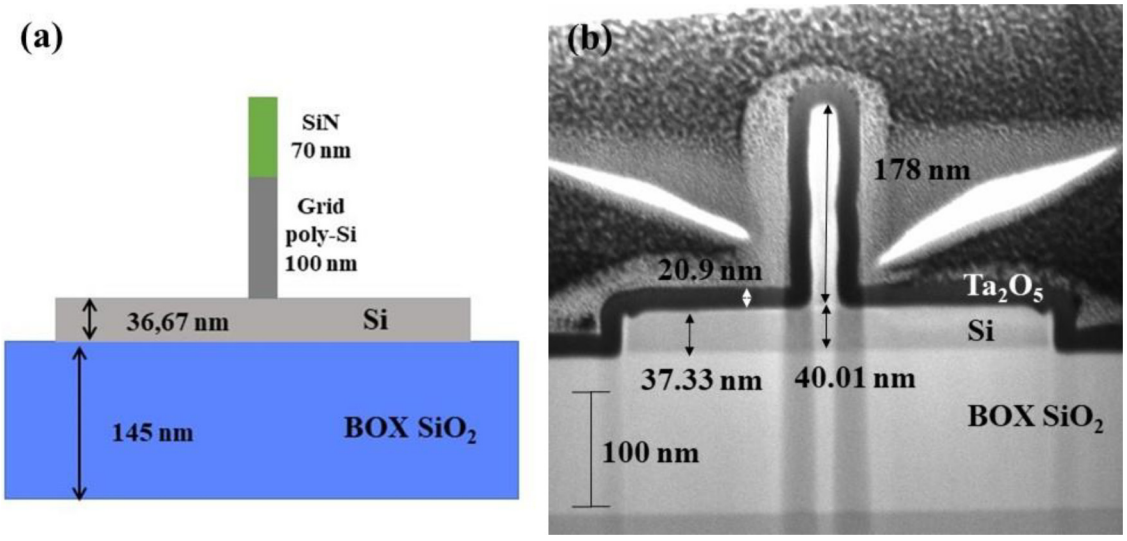

FIG. 7. (a) Schematic description of the 3D pristine structure and (b) transmission electron microscope image of a PEALD-processed 3D structure.

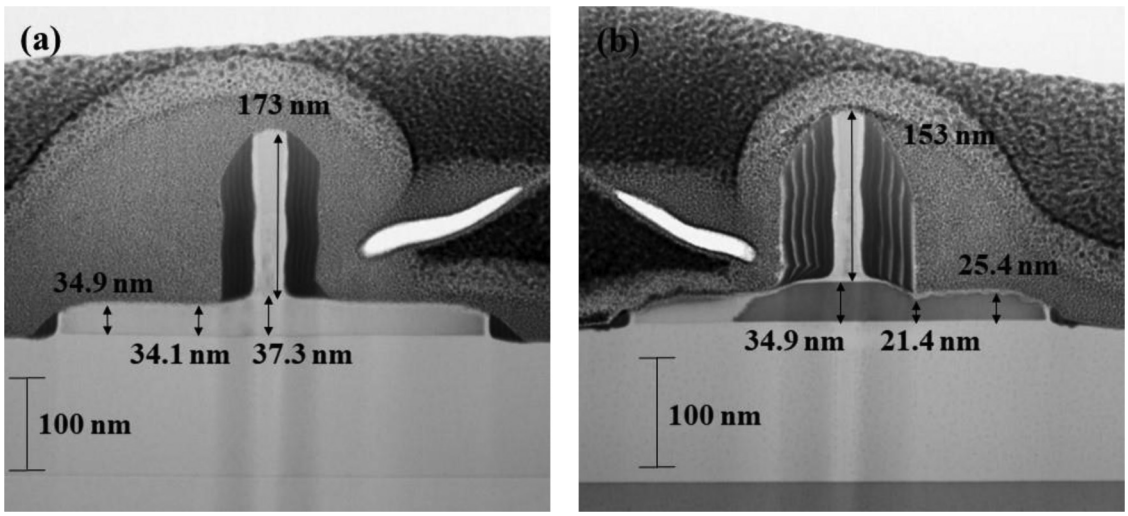

FIG. 8. Transmission electron microscope images of vertical TSD in 3D structures: (a) PEALD/quasi-ALE TSD and (b) PEALD/50 W Ar^+ sputtering (Ref. 15).

In the following, we present a proof of concept of the TSD process based on PEALD alternating with quasi-ALE. We discuss the benefits and drawbacks of this selective deposition approach, in comparison with our previously published TSD process involving PEALD alternating with directional energetic Ar^+ ionic bombardment.

Figure 6 illustrates *in situ* ellipsometric measurements during five super-cycles alternating PEALD and quasi-ALE carried out on a planar Si substrate. Each supercycle consists of 50 Ta_2O_5 PEALD cycles (leading to 4 nm Ta_2O_5), followed by 32 quasi-ALE cycles, as described in Fig. 4. It can be observed that the thickness is not restored to 0 nm at the end of the first supercycle, with selectivity with respect to a 1.3 nm-thick sublayer (the inset of Fig. 6). This is attributed to Si substrate oxidation induced by O_2 plasma exposure in the second half cycles of the PEALD process.[15] This interfacial oxide layer slightly increases to 1.6 nm at the end of the second supercycle, but does not show any further increase thereafter, and the alternate deposition/etch process reaches a stationary state at the third supercycle.

In a second phase, this five supercycle process has been transferred to 3D structures, to check the occurrence of a vertical TSD. Figure 7(a) shows a schematic description of the 3D stack used for this purpose. As expected, 5×50 Ta_2O_5 PEALD cycles (i.e.,

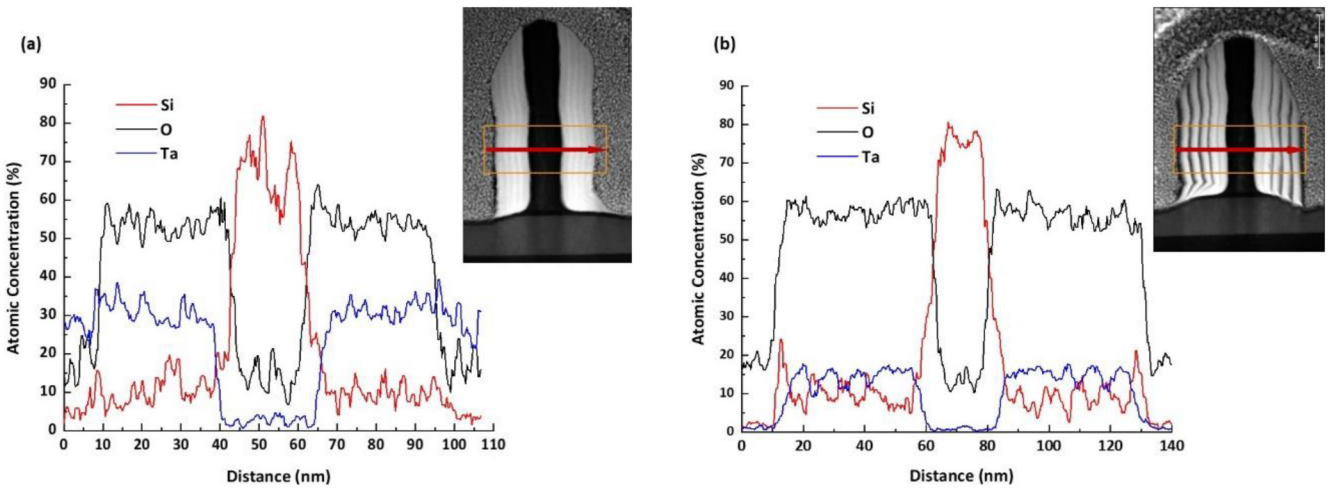

FIG. 9. EDX line scan of the 3D structures after (a) PEALD/quasi-ALE and (b) PEALD/50 W Ar^+ sputtering, showing relative Si, O, and Ta contents along the line scan.

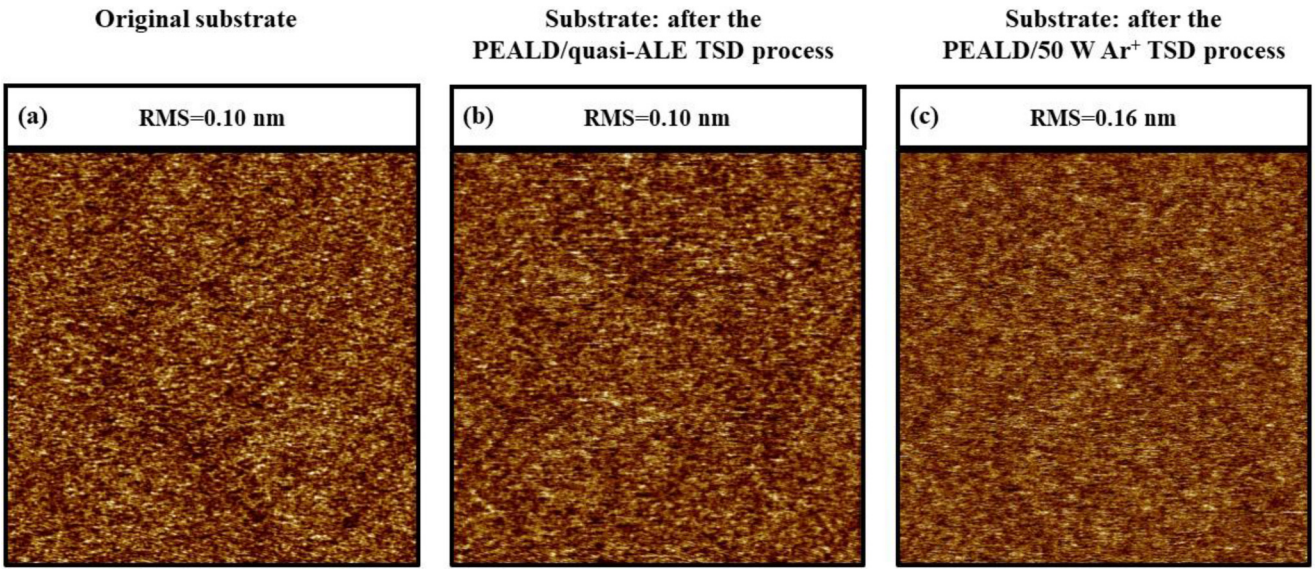

FIG. 10. Atomic force microscope images and corresponding RMS measurements: (a) a planar Si substrate, (b) after the PEALD/quasi-ALE TSD process, and (c) after the PEALD/ 50 W Ar+ sputtering TSD process.

cumulative PEALD cycles of five TSD super-cycles) lead to a smooth and conformal thin film having a uniform thickness of 20 nm [Fig. 7(b)].

Figure 8(a) shows the same structure after the five PEALD/quasi-ALE super-cycles have been carried out, according to Fig. 6. It shows the successful local deposition of Ta_2O_5 having a thickness of ca 33 nm on the vertical sidewalls, as obtained at relatively low incident kinetic energy Ar^+ bombardment (21 W bias power).

Finally, the quality of this PEALD/quasi-ALE TSD process [Fig. 8(a)] is compared with the PEALD/50 W Ar^+ sputtering TSD process without any intermediate fluorination treatment [Fig. 8(b)] that we have previously developed.[15] Figure 8(a) shows no by-product redeposition and very little damage induced by the post-fluorination 21 W Ar^+ ion exposure on horizontal surfaces, although a small erosion can be measured. Additionally, a comparison between Figs. 8(a) and 8(b) proves that the vertical coating obtained by ALD/quasi-ALE is more homogeneous than the one obtained by PEALD/50 W Ar^+ sputtering. EDX measurements carried out on both structures (Fig. 9) confirm this point. In particular, the thin vertical lines along the sidewalls in Fig. 8(b) are quite noticeable and are attributed to a redeposition of sputtered silicon species from the energetic 50 W Ar^+ bombardment of horizontal surfaces, as revealed by EDX measurements [Fig. 9(b)]. These lines are much less noticeable in Fig. 8(a), corresponding to the PEALD/quasi-ALE TSD process developed in the present work.

Moreover, AFM measurements were carried out on planar Si substrates after both TSD processes, as shown in Fig. 10. We observe a significant roughness improvement in the TSD process involving quasi-ALE. The RMS value shows a notable increase from 0.10 nm for the planar Si substrate [Fig. 10(a)] to 0.16 nm after PEALD/50 W Ar^+ sputtering [Fig. 10(c)], consistent with plasma-induced damage under heavy ionic bombardment. Conversely, the 0.10 nm RMS value measured after PEALD/quasi-ALE [Fig. 10(b)] is identical to that of the pristine substrate, despite the horizontal surface low erosion evidenced in TEM pictures [Fig. 8(a)]. These AFM results again emphasize the benefits gained from the development of a quasi-ALE process step to achieve TSD, in comparison with our previously published approach involving a 50 W energetic Ar^+ sputtering process step.

IV. SUMMARY AND CONCLUSIONS

This work shows a proof of concept for the successful vertical topographically selective deposition of Ta_2O_5 based on super-cycles alternating PEALD and quasi-ALE cycles. We have shown that the insertion of an *in situ* fluorination surface treatment allows the subsequent removal of horizontal coatings by directional ion bombardment at relatively low incident kinetic energies, thereby significantly reducing plasma-induced damage, such as roughness and/or by-product redeposition. Although work still needs to be done concerning the enhancement of selectivity of the quasi-ALE step, this process route to TSD seems very promising in the sense that all process steps are implemented in a unique reactor, making process scale-up to industrial needs quite attractive. However, this unique reactor approach also requires special attention dedicated to cross contaminations induced by fluorine species, which readily adsorb on reactor walls and are also very prompt in spontaneous degassing during subsequent processes. Further work is in progress to address this point and to promote the selectivity of quasi-ALE by strongly mitigating the incident kinetic energy of Ar^+ ions during the sputtering step.

ACKNOWLEDGMENTS

We acknowledge the financial support of LabEx Minos for the Ph.D. funding of M.J.

DATA AVAILABILITY

The data that support the findings of this study are available from the corresponding author upon reasonable request.

REFERENCES

[1]C. Bencher, Y. Chen, H. Dai, W. Montgomery, and L. Huli, Opt. Microlithogr. XXI **6924**, 69244E (2008).
[2]A. Raley *et al.*, SPIE Newsroom (11 August 2016).
[3]K. Xu *et al.*, Adv. Etch Technol. Nanopatterning II **8685**, 86850C (2013).
[4]G. N. Parsons, J. Vac. Sci. Technol. A **37**, 020911 (2019).
[5]R. Vallat, R. Gassilloud, O. Salicio, K. El Hajjam, G. Molas, B. Pelissier, and C. Vallée, J. Vac. Sci. Technol. A **37**, 020918 (2019).
[6]K. Galatsis *et al.*, Adv. Mater. **22**, 769 (2010).
[7]F. Paquin, J. Rivnay, A. Salleo, N. Stingelin, and C. Silva, J. Mater. Chem. C **3**, 10715 (2015).
[8]A. J. M. Mackus, M. J. M. Merkx, and W. M. M. Kessels, Chem. Mater. **31**, 2 (2019).
[9]W. H. Kim *et al.*, ACS Nano **10**, 4451 (2016).
[10]W.-H. Kim, H.-B.-R. Lee, K. Heo, Y. K. Lee, T.-M. Chung, C. G. Kim, S. Hong, J. Heo, and H. Kim, J. Electrochem. Soc. **158**, D1 (2011).
[11]M. F. J. Vos, S. N. Chopra, M. A. Verheijen, J. G. Ekerdt, S. Agarwal, W. M. M. Kessels, and A. J. M. Mackus, Chem. Mater. **31**, 3878 (2019).
[12]A. Mameli, B. Karasulu, M. A. Verheijen, B. Barcones, B. Macco, A. J. M. Mackus, W. M. M. E. Kessels, and F. Roozeboom, Chem. Mater. **31**, 1250 (2019).
[13]G. N. Parsons and R. D. Clark, Chem. Mater. **32**, 4920 (2020).
[14]C. Vallée *et al.*, J. Vac. Sci. Technol. A **38**, 033007 (2020).
[15]A. Chaker, C. Vallee, V. Pesce, S. Belahcen, R. Vallat, R. Gassilloud, N. Posseme, M. Bonvalot, and A. Bsiesy, Appl. Phys. Lett. **114**, 043101 (2019).
[16]Y. Kuo, J. Electrochem. Soc. **139**, 579 (1992).
[17]M. F. A. Muttalib, R. Y. Chen, S. J. Pearce, and M. D. B. Charlton, J. Vac. Sci. Technol. A **32**, 041304 (2014).
[18]D. E. Ibbotson, J. A. Mucha, D. L. Flamm, and J. M. Cook, Appl. Phys. Lett. **46**, 794 (1985).
[19]Y. Luo, *CRC Handbook of Chemistry and Physics* (CRC Press, 2009), p. 65.
[20]K. J. Kanarik *et al.*, J. Vac. Sci. Technol. A **35**, 05C302 (2017).
[21]C. Mannequin, C. Vallée, K. Akimoto, T. Chevolleau, C. Durand, C. Dussarrat, T. Teramoto, E. Gheeraert, and H. Mariette, J. Vac. Sci. Technol. A **38**, 032602 (2020).
[22]R. J. Gasvoda, Z. Zhang, S. Wang, E. A. Hudson, and S. Agarwal, J. Vac. Sci. Technol. A **38**, 050803 (2020).
[23]S. K. Song, H. Saare, and G. N. Parsons, Chem. Mater. **31**, 4793 (2019).